[16] D. A. Hill, "Human radiowave absorption from 7 to 40 MHz", in *Proc. Workshop on the Protection of Personnel Against Radiofrequency Electromagnetic Radiation*, J. C. Mitchell, Ed., USAF School of Aerospace Medicine, Aeromedical Review 3-81, Sept. 1981, pp. 170–175.
[17] H. Massoudi, C. H. Durney, and C. C. Johnson, "Comparison of the average specific absorption rate in the ellipsoidal conductor and dielectric models of humans and monkeys at radio frequencies," *Radio Sci.*, vol. 12(6S), pp. 65–72, Nov.–Dec. 1977.
[18] S. C. Kashyap and F. R. Hunt, "A low frequency (< 35 MHz) facility for biological absorption measurements," NRCC Division of Electrical Engineering Report #ERB-904, Sept. 1977.
[19] C. M. Weil, "The characteristic impedance of rectangular transmission lines with thin center conductor and air dielectric," *IEEE Trans. Microwave Theory Tech.*, vol. MTT-26, pp. 238–242, Apr. 1978. See Table I.
[20] O. R. Curzan and R. V. Garver, "Characteristic impedance of rectangular transmission lines," *IEEE Trans. Microwave Theory Tech.*, vol. MTT-12 pp. 488–495, Sept. 1964.
[21] F. M. Greene, "Development of electric and magnetic near-field probes," National Bureau of Standards (Boulder, CO) Technical Note 658, Jan. 1975
[22] F. M. Greene, "NBS field-strength standards and measurements (30 Hz to 1000 MHz)," *Proc. IEEE*, vol. 55, pp. 970–981, June 1967.
[23] S. J. Allen, private communication. Comparison between our *E*-field probe and his, performed in the 50-Ω TEM cell at the USAF School of Aerospace Medicine, San Antonio, TX.
[24] W. S. Metcalf, "Characteristic impedance of rectangular transmission lines," *Proc. Inst. Elec. Eng.*, vol. 112, pp. 2033–2039, Nov. 1965.
[25] P. Silvester, *Modern Electromagnetic Fields*, 1st edn. New York: Prentice-Hall, 1968, ch. 2, pp. 56–65 and ch. 8, pp. 260–263.
[26] M. L. Crawford, J. L. Workman, and C. L. Thomas, "Expanding the bandwidth of TEM cells for EMC measurements," *IEEE Trans. Electromagn. Compat.*, vol. EMC-20, pp. 368–375, Aug. 1978.
[27] M. L. Crawford, C. A. Hoer, and E. L. Komarek, "RF differential power measurement system for the Brooks AFB electromagnetic hazards experiments," NBS Report 9795, Apr. 1971.
[28] C. C. Johnson, C. H. Durney, P. W. Barber, S. J. Allen, and J. C. Mitchell, "Radiofrequency radiation dosimetry handbook," USAF School of Aerospace Medicine/RZP, Brooks Air Force Base, TX, Rep. SAM-TR-76-35, Sept. 1976.
[29] M. J. Hagmann, O. P. Gandhi, and C. H. Durney, "Numerical calculation of electromagnetic energy deposition for a realistic model of man," *IEEE Trans. Microwave Theory Tech.*, vol. MTT-27, pp. 804–809, Sept. 1979.
[30] S. V. Marshall, R. F. Brown, C. W. Hughes, and P. V. Marshall, "An environmentally controlled exposure system for irradiation of mice at frequencies below 500 MHz," in *Proc. 1981 IEEE Int. Symp. on Electromagn. Compat.*, 1981, pp. 99–104.
[31] D. A. Hill, "Bandwidth limitations of TEM cells due to resonances," submitted to *J. Microwave Power*.

Douglas A. Hill (M'82) received the B.Sc. degree in mathematics and physics from the University of Toronto in 1966. He then completed a Ph.D. degree at the University of British Columbia, studying microwave cyclotron resonance in p-type GaSb. From 1972 to 1974 he carried out post-doctoral research in nerve biophysics at the University of Western Ontario.

He is now with the Radiation Biology Section of the Defence Research Establishment Ottawa, working with the National Research Council of Canada, studying the biological effects of radiofrequency (RF) and microwave radiation. His research interests center around RF and microwave bioeffects dosimetry, his main project being the first measurements (in the HF band) of human whole-body RF absorption. He also advises the Canadian Department of National Defence on all aspects of RF radiation protection.

An Accurate, Unified Solution to Various Fin-Line Structures, of Phase Constant, Characteristic Impedance, and Attenuation

D. MIRSHEKAR-SYAHKAL AND J. BRIAN DAVIES, MEMBER, IEEE

***Abstract*—The analysis of several fin-line configurations (unilateral fin-line, bilateral fin-line, antipodal fin-line, and coupled fin-lines) has been completed accurately. In this unified method, propagation constant is achieved via the generalized spectral domain technique where the basis functions for the bounded and unbounded fields are chosen to be trigonometric functions and Legendre polynomials, respectively. The conduction loss and dielectric loss solution for the first time are found through a perturbation method. The conductor loss so derived is believed to be sufficiently accurate for practical purposes. Characteristic impedances of these transmission lines using tentative definitions have been presented. The CPU time on an IBM 360/65 for calculation of the mentioned parameters does not exceed five seconds if the fourth-order solution in the spectral analysis gives the required accuracy. The programs are also capable of detection of higher order modes.**

Manuscript received July 29, 1981; revised March 3, 1982.

The authors are with the Department of Electronic and Electrical Engineering, University College London, London, England, WC1E 7JE.

0018-9480/82/1100-1854$00.75 ©1982 IEEE

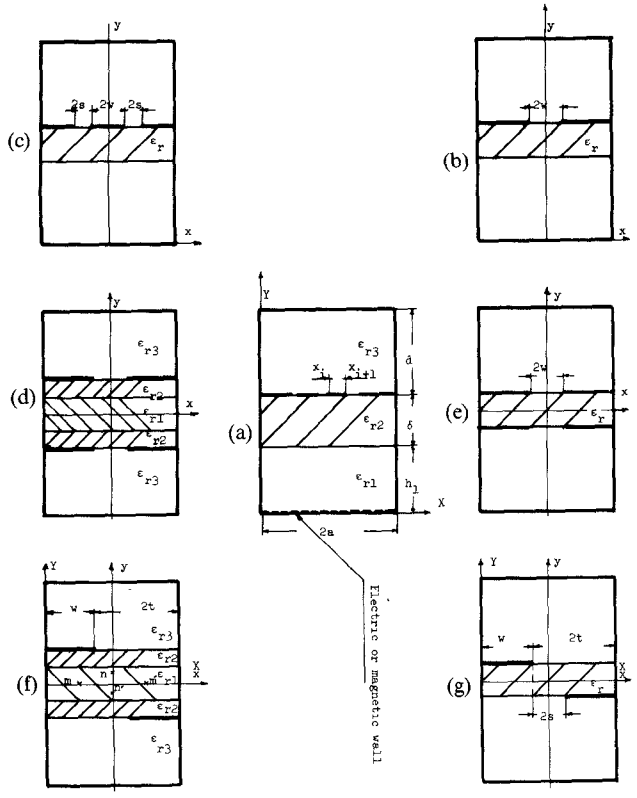

Fig. 1. General structure and various type of finlines. Numerical examples are performed for structures (a), (b), (e), and (g), where the outside cover is WG-22 waveguide and the dielectric is placed in the middle of its broad wall. In all the mentioned cases, dielectric thickness = 0.127 mm, $\epsilon_r = 2.22$, $\tan\delta_i = 2\times10^{-4}$, and $\rho = 3\times10^{-8}\ \Omega\cdot$m.

I. Introduction

WORK AT millimeter bands has presented a need for a new low-loss transmission line capable of being interfaced with other integrated components. Fin-lines, viz. metallic strips etched on plastic or ceramic substrate embodied in the trunk of the standard rectangular waveguides have been the first guiding structures fulfilling these engineering requirements. Many descriptions of these lines can be found in the literature [1], [2]. Alternative transmission lines at millimeter band are image lines [3]. Although they present lower losses than fin-line, difficulty in making them easily adapted to conventional microwave components has left them second in application to fin-lines.

In spite of scattered results in the literature on the phase constant and characteristic impedance of some fin-lines, no account of losses has yet been given. Therefore, the problem of optimum design of the fin-line, involving the conductor and dielectric losses has remained unsolved. One must bear in mind that, as the gap in fin-lines becomes smaller and smaller, the conductor loss may even exceed the microstrip loss which can be achieved at the same band as fin-line.

The technique implemented to get the phase constants of all fin-lines, including unilateral, bilateral, antipodal, and coupled fin-line, Fig. 1, is the generalized spectral domain approach developed by the authors [4], [5]. The basis functions as before [5] are chosen to be Legendre polynomials for the unbounded field components near the sharp edges of fins and/or strips. The reason for the choice of Legendre polynomials is not just because they enjoy a closed-form Fourier transformation, but they are also advantageous in computing conductor losses. This point will be clarified in Section II-B. A perturbation solution for conductor loss and dielectric loss has been given in [6] for a general microwave integrated coplanar transmission line. This is used directly in fin-lines for the same purposes.

In this analysis of fin-lines, results are compared with accurate and reliable sources of information, if available. The presented techniques are very efficient in computing, and it is believed they could be programmed for fin-lines onto a small computer, with about 30K-byte store.

II. Theoretical Background

As the method is a development of that described in [4], [6] for multilayer dielectric multistrips, a very short resumé is given below to highlight the remarks made later for individual fin-line configurations.

Consider Fig. 1(a), where the right-hand side wall (i.e., $Y = 0$), can be assumed as a magnetic wall or electric wall, and conductors, either strips or fins, are placed on one side of the dielectric as shown. This structure is a substructure of the general planar configuration shown in [4], [6]. Therefore, in view of lossless conductors and homogeneous dielectrics the following relations hold true [4], [6]:

$$\begin{bmatrix} A_2 \\ B_2 \\ C_2 \\ D_2 \end{bmatrix} = [T_{2,1}] \begin{bmatrix} A_1 \\ B_1 \\ C_1 \\ D_1 \end{bmatrix} \tag{1}$$

where

$$[T_{2,1}] = [\gamma_2 h_1]^{-1}[\gamma_1 h_1] \tag{2}$$

and A_2, B_2, C_2, D_2, A_1, B_1, C_1, and D_1 are the coefficients of potential functions in the finite Fourier domain given as follows:

$$\tilde{\psi}_i^e = A_i \sinh\gamma_{i,n} Y + B_i \cosh\gamma_{i,n} Y \tag{3}$$

$$\tilde{\psi}_i^h = C_i \sinh\gamma_{i,n} Y + D_i \cosh\gamma_{i,n} Y, \qquad i = 1,2 \tag{4}$$

where

$$\gamma_{i,n}^2 = \alpha_n^2 + \beta^2 - k_i^2 \tag{5}$$

α_n, $j\gamma_{i,n}$, β are the X, Y, Z components of wavenumber k_i in each region of dielectrics, and α_n denotes the Fourier spectrum constant given by

$$\alpha_n = \frac{n\pi}{2a}, \quad n = 0,1,2,\cdots \tag{6}$$

for unsymmetrical structures. For a structure with magnetic wall or electric wall at $X = a$, α_n becomes

$$\alpha_n = (n + 1/2)\pi/a \quad \text{or} \quad \alpha_n = n\pi/a \tag{7}$$

respectively.

From [4] and [6], the matrix $[G]$ relating E_X, E_Z, J_X, and J_Z at $y = h_1 + \delta$ and in the Fourier domain is specified by

$$\begin{bmatrix} G_{1,1} & G_{1,2} \\ G_{2,1} & G_{2,2} \end{bmatrix} \begin{bmatrix} \tilde{J}_X \\ \tilde{J}_Z \end{bmatrix} = \begin{bmatrix} \tilde{E}_Z \\ \tilde{E}_X \end{bmatrix} \tag{8}$$

where $\tilde{E}$ and $\tilde{J}$ are E and J in the Fourier domain. As

numerically proved, different arrangements of (8) submit different computing efficiencies [6]. Efficiency is measured by the number of basis functions required in each arrangement to reach the same precision in a solution. An instance of this can be seen in the microstrip problem where (8) is much more efficient than (9), while in slot relation (9) is superior

$$[G]^{-1}\begin{bmatrix}\tilde{E}_Z\\ \tilde{E}_X\end{bmatrix}=\begin{bmatrix}\tilde{J}_X\\ \tilde{J}_Z\end{bmatrix}. \tag{9}$$

It is believed that to achieve the optimum CPU time, the arrangement should be chosen in which currents and/or electric fields are to be approximated over the shortest intervals. In the proceeding work, it is thus much easier to work with (9) since usually E_X and E_Z have to be expanded over a small interval, within the gap for unilateral (Fig. 1(b) and (c)) and bilateral (Fig. 1(d) and (e)) fin-line. For some gap dimensions, the performance of (9) may not be the most efficient, but since continuity of numerical solutions is of concern, (9) has been used for all gap dimensions. In antipodal fin-line (Fig. 1(f) and (g)), (8) is advantageous for fin dimensions less than 'a', but as the fin size becomes larger than 'a', (9) yields a solution in less CPU time.

Assuming G_{ij} in (9) are known, the next step is to select expansion functions for E_X and E_Z. The expansion functions chosen throughout are Legendre polynomials for the unbounded field E_X, and sinusoids for the bounded field E_Z. The explicit expressions for the basis functions are given for each fin-line structure later in the paper. The choice of Legendre polynomials for approximation of E_X is because a) they have closed-form Fourier transform, and b) although required to approximate the unbounded singularity of E_X [7], the individual Legendre polynomials are bounded. The latter fact is actually advantageous in the computation of conductor loss where, due to the unbounded fields for an infinitely thin perfect conductor, the use of unbounded basis functions leads to unbounded conductor loss. This point is expanded later in Section II-B.

Transforming the basis functions into the Fourier domain and substituting in (9), then applying Galerkin's method and Parseval's identity, one obtains a set of homogeneous linear equations whose nontrivial solution yields phase constant of the structure in question [8].

A. Dielectric Loss

Calculation of dielectric loss is based on the assumption of low-loss dielectric materials. Therefore, a perturbation formulation developed in [6] for a general shape planar structure can be directly implemented for all fin-line configurations and the final expression is given by

$$\alpha_d=\frac{\omega\sum_i \epsilon_i \tan\delta_i \int_{S_i}|\vec{E}_0|^2\,ds}{2\,\mathrm{Re}\int_S \vec{E}_0\times\vec{H}_0^*\,\vec{ds}}. \tag{10}$$

In (10), $\vec{E}_0$ and $\vec{H}_0$ are electric and magnetic fields before introduction of dielectric loss, $\tan\delta_i$. S and S_i represent the whole cross section and dielectric sections, respectively. Since all fields are available in the transformed domain, both integrals in (10) are reduced to truncated series, greatly simplifying the computations of α_d [6].

B. Conductor Loss

The conventional formula for conductor loss of a transmission line with high conductivity conductor is given by [9]

$$\alpha_c=\frac{R_s\int_c|\vec{H}_t|^2\,dl}{2\,\mathrm{Re}\int_S \vec{E}_0\times\vec{H}_0^*\,\vec{ds}} \tag{11}$$

where R_s is surface resistance and $\vec{H}_t$ is the tangential magnetic field around the conductor periphery for lossless case. The only problem encountered in calculation of α_c is the integral

$$\int_c|\vec{H}_t|^2\,dl. \tag{12}$$

This integral is unbounded at the edge of an infinitely thin lossless strip [10], and (11) has to be used cautiously with conductor edges.

In fin-line, microstrip, and similar planar guides, field components E_X and J_Z will have $r^{-1/2}$ type singularities near any thin perfectly conducting edge. Substitution into (11) gives an unbounded value—an infinity that is a mathematical artefact. This is because, consequent on the assumption of a finite conductivity, it immediately follows that fields are everywhere bounded—even in geometric limit of the zero-thickness strip with sharp edges. Bounded fields will yield a bounded value for attenuation, (assuming only a nonzero net power flow).

Of course, the assumption of a finite conductivity together with a zero-thickness conductor must be interpreted carefully at microwave frequencies. It must be assumed that the conductor thickness is much greater than the skin depth; this is usually true in practice at microwave frequencies, and needs to be true for the perturbation approach of (11) to be valid. For validity of the field analysis between the conductor regions, 'zero thickness' must be taken as meaning that the conductor thickness is much less than any structural dimensions.

To describe the procedure used for the computation of conductor loss, suppose that either E_X or J_Z is expanded as a truncated series of Legendre polynomials, (in Section III-A, (18) gives the choice for unilateral fin-line; J_Z would be similarly expanded for microstrip)

$$E_x=\sum_{m=1}^{P} a_m \boldsymbol{P}_{2(m-1)}(x/w). \tag{13}$$

Limiting the number of terms to P means that spatial discrimination in the X direction is limited to w/P; the essential singularity of

$$\int_0^w \frac{dx}{(w-x)}$$

is replaced by the finite

$$\int_0^{w(1-1/P)} \frac{dx}{(w-x)}.$$

One can then ask the question: How does the computed result for attenuation depend on P the number of terms? Tests with microstrip have shown that increasing the highest polynomial order from 4 to 12 gives an attenuation higher by about 10 percent. The structure chosen was the microstrip in [5, fig. 6(b)], with $w/d = 2$ and using 150 Fourier terms, where the resulting attenuation increases from 0.59 to 0.64 dB/m. Although not conclusive, it does indicate the reasonable convergence, and so the usefulness, of the conductor-loss calculation. Formula (11) does, of course, depend on satisfying the inequalities

skin depth $\ll$ strip thickness $\ll$ other structural dimensions.

C. Characteristic Impedance

Due to hybrid wave propagation in fin-lines, a unique definition for characteristic impedance does not exist. However, the most common and useful definition is based on the voltage/power relationship, where the voltage is measured from one fin edge to another. In the configuration analyzed, for single fin-line, the characteristic impedance Z_0 is given by

$$Z_0 = V^2/P \tag{14}$$

while for coupled lines

$$Z_0 = 2V^2/P \tag{15}$$

where

$$V = \int_{\text{over gap}} E_x dx \tag{16}$$

$$P = \text{Re} \int_S \vec{E}_0 \times \vec{H}_0^* \, \vec{ds} \tag{17}$$

where S is the whole cross section of the guide.

III. Applications

The technique described above is now applied to various examples of fin-line, outlined as follows.

A. Unilateral Fin-Line

Fig. 1(b) shows a generic cross section of unilateral fin-line where h_1 may be different from d (see Fig. 1(a)). This case is similar to shielded slot analyzed by the authors in [5]. Therefore, all the relations given for G_{ij} can be directly implemented in a computer program to analyze the unilateral fin-line. Notice that for this structure, the G_{ij} elements of (8) correspond to consideration of an electric wall at $y = 0$; in relation (1) $B_1 = C_1 = 0$. As discussed above, basis functions are given by

$$\left.\begin{aligned} E_x &= \sum_{m=1}^{P} a_m P_{2(m-1)}(x/w) \\ E_z &= \sum_{m=1}^{Q} b_m \sin m\pi(x/w) \end{aligned}\right\}, \quad |x| < w \quad \text{at} \quad y = h_1 + \delta \tag{18}$$

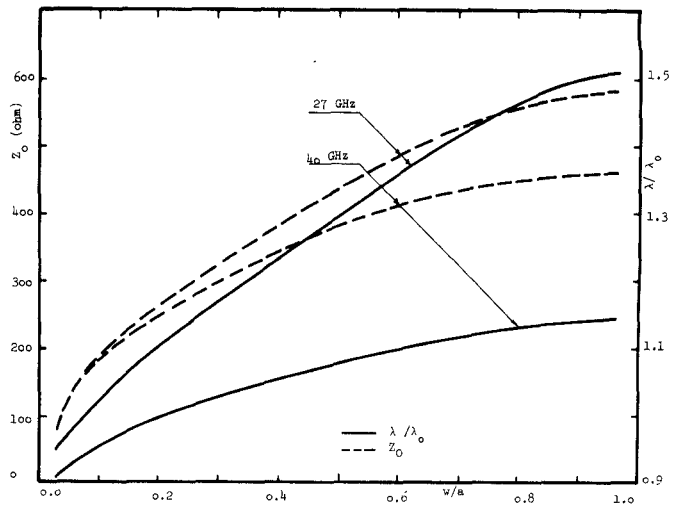

Fig. 2. Normalized wavelength λ/λ_0 and characteristic impedance Z_0 of unilateral finline (Fig. 1(b)).

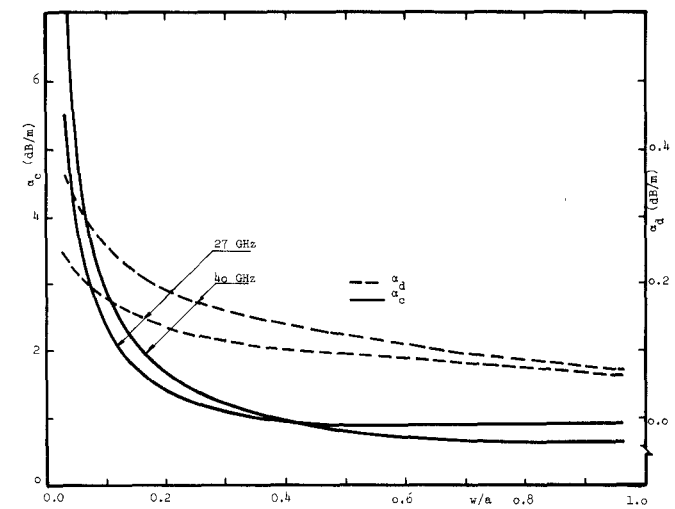

Fig. 3. Conductor loss α_c and dielectric loss α_d of unilateral finline (Fig. 1(b)).

where $P_{2(m-1)}$ represents Legendre polynomials of degree $2(m-1)$.

The computer results for propagation constant, characteristic impedance, dielectric loss, and conductor loss for a fin-line whose dielectric substrate is symmetrically placed within WG-22 waveguide are given in Fig. 2 and Fig. 3 over *Ka*-band. To check the speed of convergence and the accuracy of the applied method, it was tested against [11] where a very close agreement after considering $P = Q = 4$ was achieved.

For unilateral fin-line with very low dielectric constant, $\epsilon \simeq 1.0003$ and with large gap $w/a \simeq 0.98$, the normalized wavelength, characteristic impedance, and conductor loss are compared with those of empty guide supporting the TE_{10} mode (Table I). The close agreement of values of those two guides indeed supports the accuracy of the presented numerical technique.

From Fig. 3, it is seen that, due to heavy concentration of fields near the small gap, the conductor loss and dielectric loss are not very low. Nevertheless, for a 400-μm gap, commonly etched, the total loss is around 2.5 dB/m over the whole *Ka*-band.

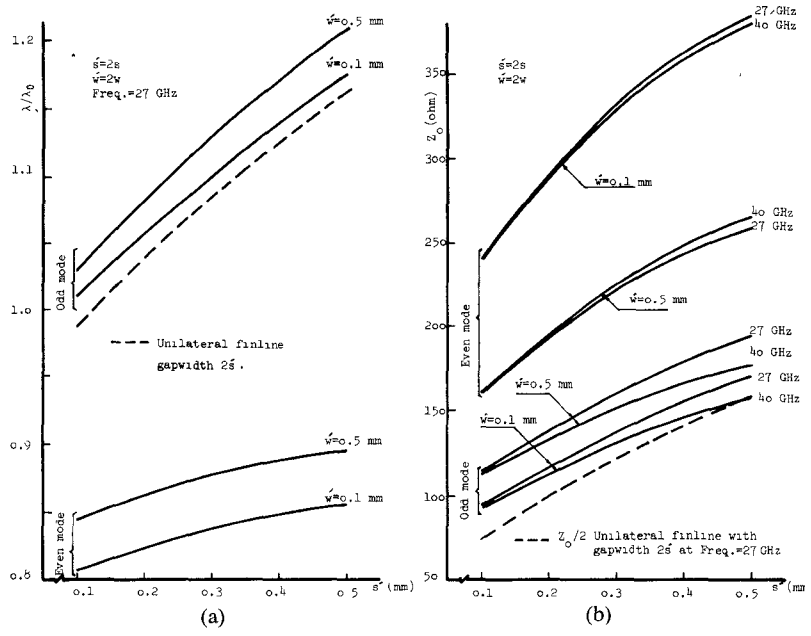

Fig. 4. (a) Normalized wavelength λ/λ_0 and (b) characteristic impedance Z_0 of even and odd mode of coupled finline (Fig. 1(c)).

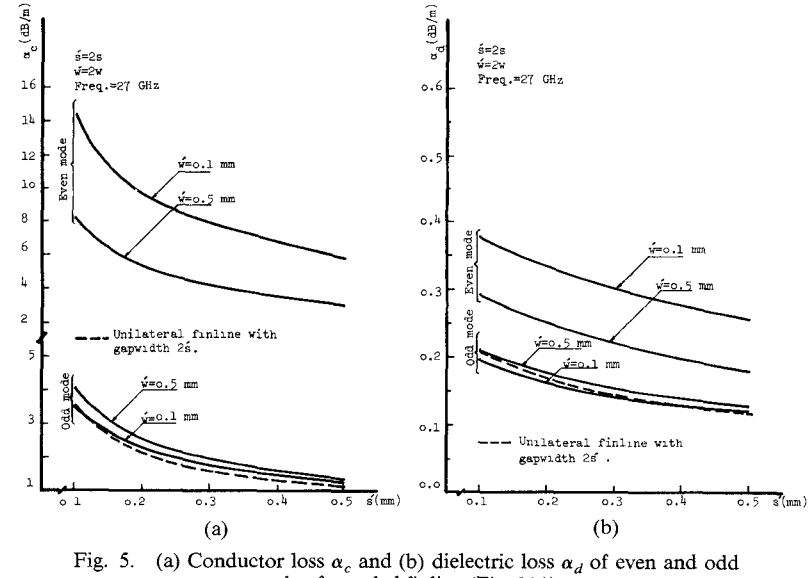

Fig. 5. (a) Conductor loss α_c and (b) dielectric loss α_d of even and odd mode of coupled finline (Fig. 1(c)).

TABLE I
A COMPARISON BETWEEN EMPTY WG-22 WAVEGUIDE PARAMETERS (*) AND THOSE OF UNILATERAL FIN-LINE WITH $w/a = 0.98$, $\epsilon_r = 1.0003$ AND $\rho = 3\times10^{-8}\Omega\cdot$m

Freq. GHz	λ_g/λ_0	$Z_0(\Omega)$	α_c dB/m
27	1.598*	599.76*	0.937*
	1.603	604.24	0.946
40	1.176*	440.54*	0.675*
	1.177	443.78	0.671

B. Coupled Coplanar Fin-Lines

This structure, Fig. 1(c), has recently been used in making a quadriphase fin-line modulator [12] where the parameters have been obtained empirically. However, with the introduced general technique, determination of the required parameters of the coupled coplanar fin-lines is not difficult. The only alteration to be made in the unilateral fin-line analysis is the change of basis functions given by

$$\left.\begin{aligned} E_x &= \sum_{m=1}^{P} a_m \boldsymbol{P}_{m-1}[(x-w-s)/s] \\ E_z &= \sum_{m=1}^{Q} b_m \sin[m\pi(x-w)/2s] \end{aligned}\right\},$$

$$w < x < w+2s \quad \text{at} \quad y = h_1 + \delta. \tag{19}$$

For the 'odd mode' (defined here as having E_z an odd function of x and E_x an even function) the basis functions are correspondingly defined for negative x. The 'even

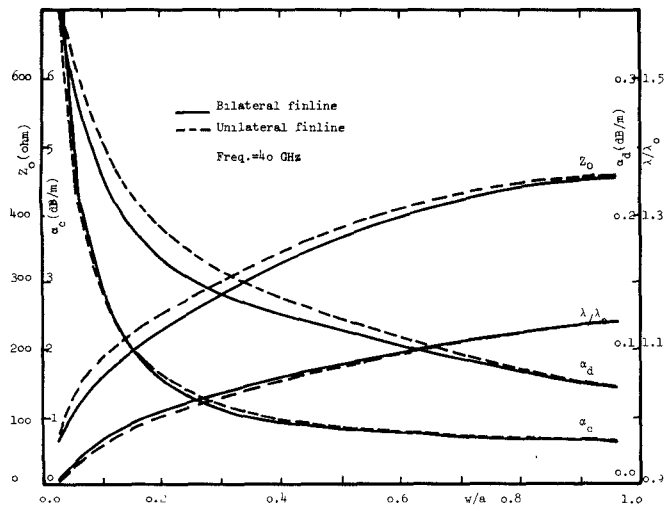

Fig. 6. A comparison between unilateral finline (Fig. 1(b)) and bilateral finline (Fig. 1(e)).

mode' has E_z an even function of x and E_x an odd function.

Figs. 4 and 5 illustrate the results of λ/λ_0, Z_0, α_c, and α_d versus slot width for two different separations of slots at a frequency of 27 GHz. The coupled coplanar fin-line as before is considered in WG-22 waveguide. A comparison of the parameters of the odd mode is carried out with those of unilateral fin-line whose slot width is twice the value of each slot. At the limit, as the separation between the two slots becomes zero, the coupled coplanar fin-line approaches the mentioned unilateral fin-line. From the given curves, the approach of parameters of the coupled line to the mentioned single line is not always monotonic but one can see their general consistency.

C. Unilateral Fin-Line and Bilateral Fin-Line as Coupled Line

Conventional and more general forms of bilateral fin-line are shown in Fig. 1(e) and (d). By symmetry about the x-axis, the analysis can be carried out just for one half of the structure. Considering a magnetic wall at $y = 0$, the $[G]$ matrix in (8) is obtained by substituting $A_1 = D_1 = 0$ in (1). This change in (1) corresponds to exchange of sinh by cosh and vice versa for all field relations in the first dielectric region, for the case of electric wall symmetry plane at $y = 0$, equivalent to Fig. 1(b) [4]. Therefore, the computer program developed for unilateral fin-line can be directly applied to the bilateral fin-line with some minor modification. The computer results for a conventional bilateral fin-line embodied in WG-22 waveguide have been illustrated in Fig. 6. A comparison of this line with unilateral fin-line of the same category, Figs. 2 and 3, reveals only a small change in the values of the associated parameters from one line to another. However, this observation may not be true for a substrate with greater thickness. Another feature of bilateral fin-line is its flexibility in being used as a pair of coupled lines, i.e., two coupled unilateral fin-lines. For the analysis of this aspect of unilateral fin-line, programs developed for the unilateral fin-line and bilateral fin-line can be called into service provided that the characteristic impedances for the even and odd modes are now defined through relation (15).

D. Antipodal Fin-Line

Cross sections of antipodal fin-lines have been shown in Fig. 1(g) and (f), where—in the latter—the structure is more general than Fig. 1(g). Note that in these two figures, there are distinct x, y axes and X, Y axes; this simplifies the equation presentation.

It is assumed that both structures have 180° rotational symmetry. This symmetry permits the solution for the fields to be expressed in a particular arrangement of even and odd symmetry, although the antipodal fin-line structure does not enjoy the simpler reflection symmetries about a plane, like those in unilateral and bilateral fin-lines. To find the solution, consider the potential functions in the space domain for the first dielectric region which, (from (3), (4), and (6)), are given as follows:

$$\psi^e(X,Y) = \sum_{n=0}^{\infty} (A_1 \sinh \gamma_{1,n} Y + B_1 \cosh \gamma_{1,n} Y) \sin \alpha_n X \tag{20}$$

$$\psi^h(X,Y) = \sum_{n=0}^{\infty} (C_1 \sinh \gamma_{1,n} Y + D_1 \cosh \gamma_{1,n} Y) \cos \alpha_n X. \tag{21}$$

For two points m and m' equally distant from 0 and on the X-axis, the following relations hold (Fig. 1(f)):

$$\psi^{(e,h)}(X,0) = \psi^{(e,h)}(2a - X,0) \tag{22}$$

provided that in (20) and (21) B_1 and D_1 are given by

$$B_1 = 0 \qquad \text{for } n = 0,2,4,6,\cdots$$
$$D_1 = 0 \qquad \text{for } n = 1,3,5,7,\cdots. \tag{23}$$

A similar argument for equally distant points n and n' on the y-axis leads to the following conclusion in (20) and (21):

$$A_1 = 0 \qquad \text{for } n = 1,3,5,7,\cdots$$
$$C_1 = 0 \qquad \text{for } n = 0,2,4,6,\cdots. \tag{24}$$

Therefore, as n takes $0,1,2,\cdots$, the right-hand side of (1) changes alternately between the following matrices:

$$\begin{vmatrix} 0 \\ B_1 \\ C_1 \\ 0 \end{vmatrix} \quad \text{and} \quad \begin{vmatrix} A_1 \\ 0 \\ 0 \\ D_1 \end{vmatrix}. \tag{25}$$

Hence, having found $[G]$ matrices corresponding to the above situations, their combination gives the required $[G]$ matrix of the antipodal fin-line. But the $[G]$ matrices corresponding to (25) are already available as the $[G]$ matrix of unilateral fin-line and $[G]$ matrix of bilateral fin-line with magnetic wall considered at the y-axis. Therefore, the solution of the antipodal fin-line by combining the two programs of the previous structures are now accessible provided that the basis functions are chosen as below

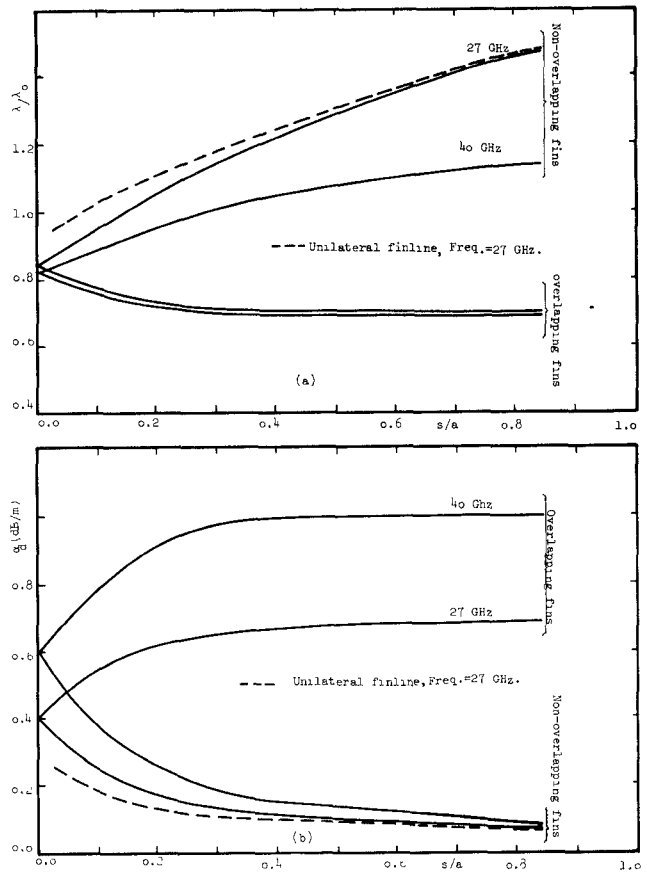

Fig. 7. (a) Normalized wavelength and (b) dielectric loss of antipodal finline (Fig. 1(g)).

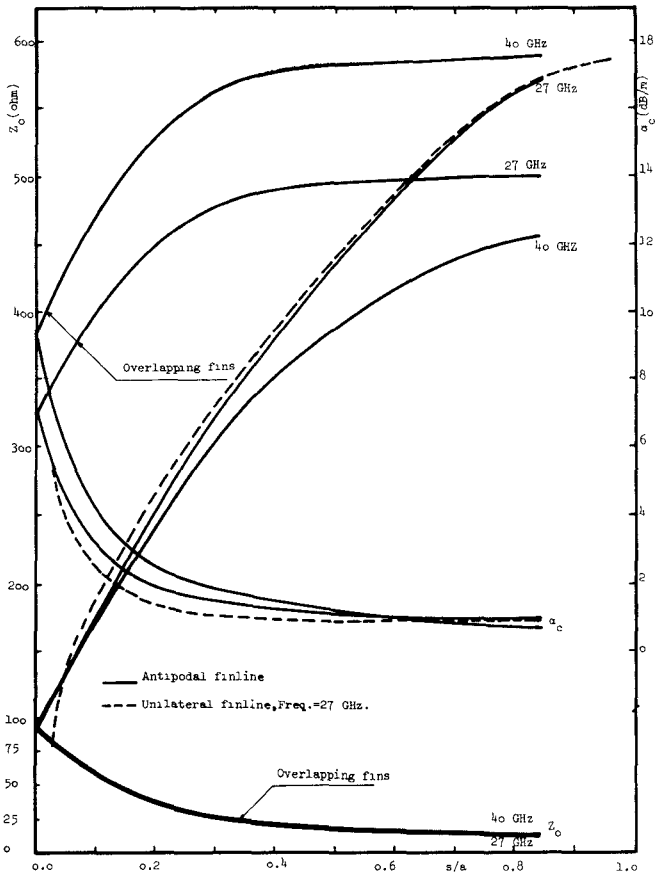

Fig. 8. Conductor loss α_c and characteristic impedance Z_0 of antipodal finline (Fig. 1(g)).

TABLE II
$2s = 3$ mm, $\delta = 0.127$ mm, $\epsilon_r = 2.22$, $\rho = 3\times10^{-8}\Omega$m, and $\tan\delta_i = 2\times10^{-4}$

	TEM Approx.			Spectral Domain		
Freq. GHz	Z_0	α_c	α_d	Z_0	α_c	α_d
27	10.77	15.0	0.73	10.05	14.0	0.69
40	10.77	18.5	1.08	10.51	17.5	1.00

(Fig. 1(f)):

$$\left.\begin{aligned} E_X &= \sum_{m=1}^{P} a_m \boldsymbol{P}_{m-1}[(X-w-t)/t] \\ E_Z &= \sum_{m=1}^{Q} b_m \sin\frac{m\pi}{2t}(X-w) \end{aligned}\right\}, \quad w < X < 2a \quad \text{at} \quad Y = h_1 + \delta. \tag{26}$$

By means of this developed method, α_c, α_d, λ/λ_0, and Z_0 of an antipodal fin-line with $h_1 = 0$ (Fig. 1(g)) have been computed and shown in Figs. 7 and 8. From these results and their comparison with unilateral fin-line results, Figs. 2 and 3, it is concluded that without overlap of the two fins, parameters of the antipodal, unilateral, and bilateral fin-lines are not significantly different. But as the fins start overlapping each other, the antipodal parameters vary substantially and are like those of parallel plate waveguide in which a TEM wave propagates. To substantiate the latter argument, α_c, α_d, Z_0 of the antipodal fin-line at large overlapping have been contrasted to those of parallel plate waveguide with width equal to $2s$ (Table II). In this comparison, parameters of finite width parallel plate waveguide have been derived, assuming that the fringing fields are negligible and it supports the TEM wave with the following relations [9]:

$$Z_0 = 1/v_p C \tag{27}$$

$$\alpha_c = 4.23 R_s / Z_0 s \tag{28}$$

$$\alpha_d = 4.23\omega\tan\delta_i / v_p \tag{29}$$

where

$$C = 2\epsilon_0\epsilon_r s/\delta \tag{30}$$

$$v_p = 1/\sqrt{\mu_0\epsilon_0\epsilon_r}. \tag{31}$$

Indeed, a close agreement is seen from Table II between the accurate solutions of the given antipodal fin-line and its approximate TEM model as s/a is large. Thus relations (27)–(31) may be used for approximate solution of antipodal fin-line with largely overlapped fins. As far as characteristic impedance is concerned, in the antipodal fin-lines the definition (14) has been used. For nonoverlapped fins, the voltage is measured from one fin edge to another, and for the overlapped fins just $E_y(x, y)$ at $x = 0$ is integrated

over the dielectric thickness as the substitution for the voltage.

IV. Conclusions

A unified method for the calculation of phase constant, characteristic impedance, dielectric loss, and conductor loss of fin-lines has been introduced. The method is in fact an application of the general analysis given by the authors for multilayer multiconductor planar transmission line [4]. Since the technique includes use of the spectral domain in determination of electric and magnetic fields, the computations of all parameters for any fin-line presented in this paper does not take more than five seconds on an IBM 360/65 if an accuracy of 0.1 percent for phase constant is acceptable. This is typical for $P = Q = 4$ in (18), (19) or (26). For the first time, dielectric loss and conductor loss, (taking account of dispersion), have been computed, in fact using a perturbation technique. For maximum advantage, particularly for achieving the conductor loss, the basis functions are chosen to be Legendre polynomials for fields that are singular near the 180° conductor edges and trigonometric functions for fields that are bounded at the same edge. This is in contrast to the use of singular basis functions [13] where loss has not been considered. The parameters of unilateral, bilateral, antipodal, and coupled fin-lines built in WG-22 waveguide were computed and compared against each other. Very close agreement was seen as the method was tested against [11] for the phase constant of unilateral fin-line. For characteristic impedance and conductor loss, the results of unilateral fin-line with very small fins were contrasted with those of empty waveguide and as expected a close connection between them was seen. An approximate solution to the antipodal fin-line with large overlapped fins has also been presented, showing agreement with the general techniques. Specially, this comparative study supports the approximations assumed for the calculation of conductor loss. The higher order mode in each discussed structure can be obtained easily without any change in programming. The developed programs for the analyzed fin-lines could be adapted to other fin structure by further modifications.

Acknowledgment

The work has been supported by Philips Research Laboratory, Redhill, England, in connection with a program sponsored by D. C. V. D., Procurement Executive, Ministry of Defence.

References

[1] P. J. Meier, "Integrated fin-line millimeter components," *IEEE Trans. Microwave Theory Tech.*, vol. MTT-22, pp. 1209–1216, Dec. 1974.

[2] P. J. Meier, "Millimeter integrated circuits suspended in the *E*-plane of rectangular waveguide," *IEEE Trans. Microwave Theory Tech.*, vol. MTT-26, pp. 726–733, Oct. 1978.

[3] R. M. Knox, "Dielectric waveguide microwave integrated circuits—An overview," *IEEE Trans. Microwave Theory Tech.*, vol. MTT-24, pp. 806–814, Nov. 1976.

[4] J. B. Davies and D. Mirshekar-Syahkal, "Spectral domain solution of arbitrary coplanar transmission line with multilayer substrate," *IEEE Trans. Microwave Theory Tech.*, vol. MTT-25, pp. 143–146, Feb. 1977.

[5] D. Mirshekar-Syahkal and J. B. Davies, "Accurate solution of microstrip and coplanar structures for dispersion and for dielectric and conductor losses," *IEEE Trans. Microwave Theory Tech.*, vol. MTT-27, pp. 694–699, July 1979.

[6] D. Mirshekar-Syahkal, "Analysis of uniform and tapered transmission lines for microwave integrated circuits," Ph.D. thesis, University of London, 1979.

[7] R. Mittra and S. W. Lee, *Analytical Techniques in the Theory of Guided Waves*. New York: Macmillan, 1971.

[8] T. Itoh and R. Mittra, "A technique for computing dispersion characteristics of shielded microstrip lines," *IEEE Trans. Microwave Theory Tech.*, vol. MTT-22, pp. 889–891, Oct. 1974.

[9] R. F. Harrington, *Time Harmonic Electromagnetic Fields*. New York: McGraw-Hill, 1968.

[10] R. Pregla, "Determination of conduction losses in planar waveguide structures," *IEEE Trans. Microwave Theory Tech.*, vol. MTT-28, pp. 433–434, Apr. 1980.

[11] E. Yamashita and K. Atsuki, "Analysis of microstrip-like transmission lines by nonuniform discretization of integral equations," *IEEE Trans. Microwave Theory Tech.*, vol. MTT-24, pp. 195–200, Apr. 1976.

[12] E. Kpodzo, K. Shunemann, and G. Begmann, "A quadriphase fin-line modulator," *IEEE Microwave Theory Tech.*, vol. MTT-28, pp. 747–752, July 1980.

[13] L. P. Schmidt, Tatsuo Itoh, and Holgar Hofman, "Characteristics of unilateral fin-line structures with arbitrary located slots," *IEEE Trans. Microwave Theory Tech.*, vol. MTT-29, pp. 352–355, Apr. 1981.

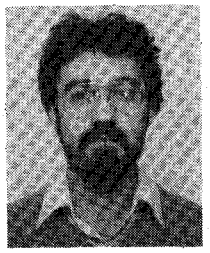

D. Mirshekar-Syahkal was born in Tehran, Iran, in 1951. He received the B.Sc. degree in electrical engineering from Tehran University, Iran, in 1974, the M.Sc. degree in microwaves and modern optics from University of College, London, England, in 1975, and the Ph.D. degree in electrical engineering in 1979.

Since 1979, he has been Research Associate at University College, London, England, where he has been working on millimeter-band planar transmission lines and on nondestructive recognition and evaluation of fatigue cracks in metal by electromagnetic techniques.

J. Brian Davies (M'73) was born in Liverpool, England in 1932.

From Jesus College, Cambridge, England, he received the degree in mathematics in 1955. From the University of London, England, he received the M.Sc. degree in mathematics, the Ph.D. degree in mathematical physics, and the D.Sc. (Eng.) degree in engineering in 1957, 1960, and 1980, respectively.

From 1955 to 1963, he worked at the Mullard Research Laboratories, Salfords, Surrey, England, except for two years spent at University College, London England. In 1963, he joined the staff of the Department of Electrical Engineering, University of Sheffield, England. Since 1967, he has been on the staff at University College, London, where he is Reader in electrical engineering. From 1971 to 1972, he was a Visiting Scientist at the National Bureau of Standards, Boulder, CO. His research work has been with problems of electromagnetic theory, especially those requiring computer methods of solution, but recently has extended into field problems in acoustic microscopy.

Dr. Davies is a member of the Institute of Electrical Engineers, London, England.